

Electronic Supplementary Information for:

Hydrodynamic chromatography - inductively coupled plasma mass spectrometry, with post-column injection capability for simultaneous determination of nanoparticle size, mass concentration and particle number concentration.

D. John Lewis

jl900cc@talktalk.net

Food and Environment Research Agency, Sand Hutton, York, YO41 1LZ.

ES-1 Configuration of HDC-PCi-ICP-MS interface components

Although the major components used in the HDC-PCi-ICP-MS were off-the-shelf items, their configuration into a working system hinged on two things; i) the ability to establish a reproducible and robust zone-of-mixing for the OC eluent and the PC injection solution; and ii) a stable, noise-free interface between the zone-of-mixing and the ICP-MS. Once these challenges had been addressed, it was hoped that it would be relatively straight forward to apply the system to the measurement of the various parameters.

Optimisation of OC and PC flow mixing.

In order to get efficient and reproducible mixing of the OC and PC liquids, a number of different designs of mixing block were investigated. The simplest were T-pieces made of PTFE, which were standard items from the ICP-MS consumable list but, where necessary, were adapted in-house. Figure ES-1a presents the T-piece configured so as to have the confluence of the OC (blue tubing) and PC (red tubing) flows occurring head-on, with the mixed flow passing at right angles through the block, through to the ICP-MS *via* the white tubing. Figure ES-1b shows the configuration where the OC and PC flows meet at right angles to each other, before passing on to the ICP-MS. In addition to this, the diameters of the various inlet and outlet ports were further adapted, in an attempt to either constrict or increase the relative flows and volumes of the liquids encountering each other. Unfortunately, none of the above configurations resulted in a consistent mixing of the two flows, as indicated by the increased levels of noise observed in the chromatographic baseline.

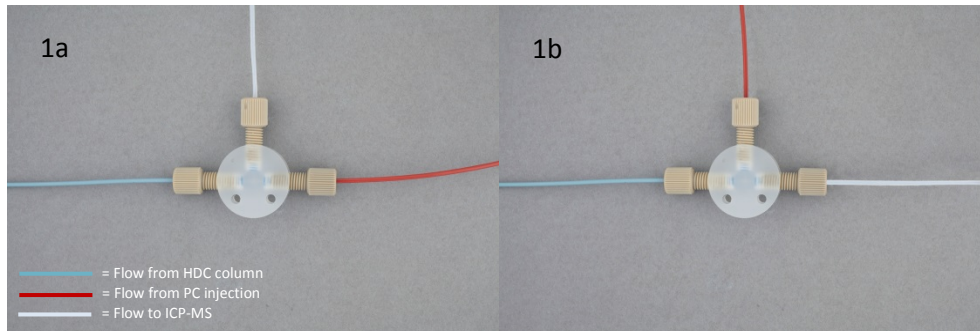


Figure ES-1. Configuration of the PTFE T-piece mixing block

In order to try and improve this situation, two Y-piece units were investigated, one from a Perkin Elmer FIAS system (Part number B0507962, *Perkin-Elmer, Beaconsfield, UK*), and the other taken from a UPLC-MS system (Part number U-466, *Crawford Scientific Ltd, Strathaven, UK*).

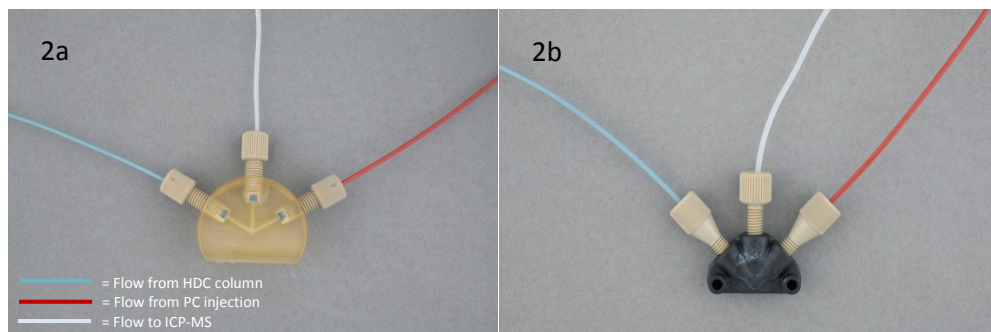


Figure ES-2.

Figure ES-2. Configuration of the two Y-piece mixing blocks.

Perkin Elmer mixing block: Figure ES-2a shows the two incoming flows meeting at approximately 90° before turning virtually back on themselves to pass through the outlet port. In addition to this, it was hoped that a void volume at the point where the two fluids meet, which had been specifically designed to efficiently mix reagents in the FIAS system, might allow time for them to properly mix before passing on

to the detector. Unfortunately, although allowing effective mixing of the liquids, the void volume was such that it had a negative impact on the quality of the chromatographic peak eluting from the column, and gave a slightly noisier signal.

Upchurch Scientific ‘low swept volume’ mixing block: Figure ES-2b shows that this unit has a similar inlet/outlet configuration, but with its low swept volume (2.2 μl), had a virtually indiscernible impact on the quality of the chromatographic peak. **For this reason, all data in the main report was obtained using this item to mix the OC and PC flows.**

Optimisation of the OC / PC flow rates:

As the OC flow rate was fixed at 1.7 ml min^{-1} , based on the manufacturer guidelines for optimal HDC separation, various PC flow rates were investigated. If too low ($<0.2 \text{ ml min}^{-1}$), the OC flow dominated access to the mixing area within the Y-piece, resulting in a relatively noisy signal being obtained from the flow-injected analyte. Flow rates greater than 1 ml min^{-1} resulted in a significant reduction in the response obtained from the eluting nanoparticle peak due to the diluting effect of the increased volume of liquid passing through the system. An optimal PC flow rate was found to be 0.7 ml min^{-1} , based on the quality of the PC-standard peak (in terms of both peak shape and signal noise), and was used for all experiments discussed in the main paper.

Interfacing the HDC-PCi flow to the ICP-MS:

A PTFE T-piece was placed immediately after the Y-piece mixing block, from which the nebuliser of the ICP-MS was able to take up solution by natural aspiration. Excess liquid flowed to waste by gravity, *via* tubing with a much larger internal diameter. It was found that the ICP-MS signal was much quieter when neither of these flows was pumped. The length of the tubing between the Y-piece mixing block, the T-piece and the nebuliser was kept as short as was practicably possible so as to keep peak-broadening to a minimum. It also helped the performance of the nebuliser by reducing in-tubing drag during natural aspiration. Figure ES-3 shows the component parts of the HDC-PCi-ICP-MS interface.

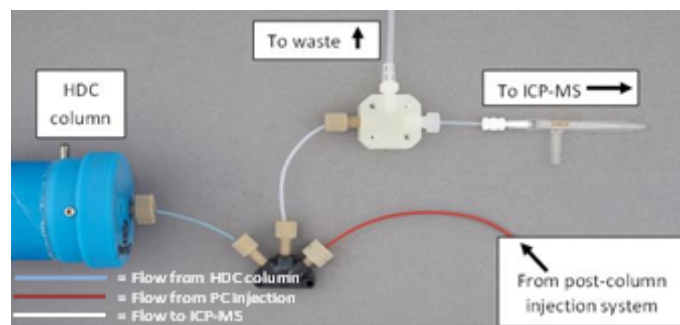


Figure ES-3. Configuration of the post-column interface components for HDC-PCi-ICP-MS.

Optimisation of the nebuliser operation settings:

As the transfer of the eluent mixture to the ICP-MS occurred as a result of the nebuliser's natural aspiration, the gas flow settings were very different to those used if operating the instrument under normal 'pumped' conditions. Optimisation of the gas flows was achieved by naturally aspirating a tune solution (containing the elements of interest, at about 10 ng ml^{-1} , made up in mobile phase) into the plasma, and then tuning the nebuliser and make-up gases so that the back-ground signal (48 m/z) was minimised, and the analyte signal maximised. 48 m/z was chosen because it had been observed to be particularly prone to the production of polyatomic interferences (based on S, N and O), so was useful as an indicator of the conditions within the plasma. As best-practise, it was helpful to also monitor at least two isotopes for each of the elements of interest, *e.g.*, for silver, monitor Ag^{107} and Ag^{109} , when altering the plasma gas flows. A constant ratio of the two isotopes confirmed that increases in the monitored signal was most likely to be due to improved analyte ionisation or transfer rather than the production of a polyatomic interference within the changing plasma. This approach was also used when performing analyses, because monitoring at least two isotopes allowed the identity of eluting peaks to be confirmed post-run.

ES-2 ICP-MS operating parameters

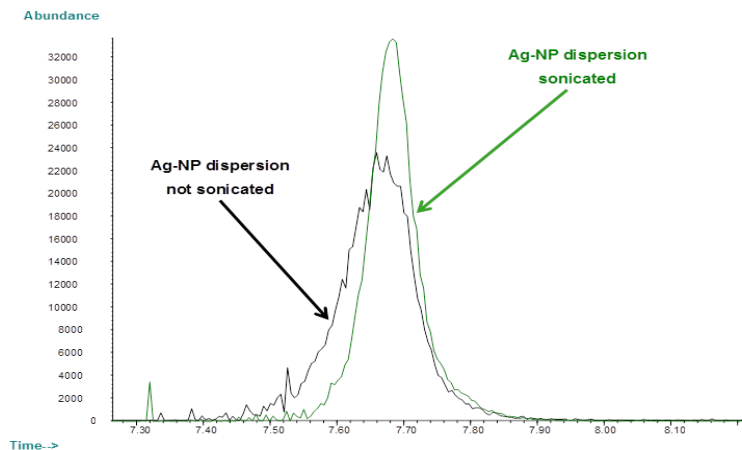
Table ES-1 Instrument parameters for the ICP-MS

Parameter	Setting
RF power	1600W
Reaction cell mode	On: He gas: 4.9 mL/min
Nebulizer pump	Natural aspiration
Nebulizer gas flow:	
Carrier gas	1.09 L/min
Make-up gas	0.26 L/min
Sample depth	10 mm
S/C temperature	2 °C
Extract 1	0 V
Extract 2	-100 V
Omega Bias-ce	-18 V
Omega Lens-ce	0.8 V
Cell entrance	-36 V
OctP RF	190 V
OctP Bias	-7 V
Isotopes monitored	^{46}Ti , ^{47}Ti , ^{48}Ti , ^{49}Ti , ^{107}Ag , ^{109}Ag and ^{197}Au
HDC column flow	1.7 ml min ⁻¹
Post-column column flow	0.7 ml min ⁻¹

ES-3 Preparation of PVP-Ag nanoparticle material.

The improved peak symmetry, following sonication, indicates that the added energy has caused disruption of larger-sized structures within the original dispersion, resulting in a smaller, more mono-disperse system.

Figure ES-4. Chromatograms showing the effect of sonication on the silver nanoparticle dispersion



This was supported by disc centrifugation data obtained on the same samples, with the polydispersity index (PDI) value being reduced to nearly 1 (where '1' indicates a totally monodisperse system), and is in line with the findings of Loeschner et al.¹⁷ when they described the particle distribution as not being monodisperse, *i.e.*, exhibiting a bimodal size distribution.

Table ES-2. Disc centrifugation data showing effect of sonication on the silver nanoparticle dispersion

Sample replicates = 3	Average size (nm)	PDI
Unsonicated dispersion	39.2	1.98
Sonicated dispersion	33.0	1.14

Figure ES-5 a to c: disc centrifugation data showing:

Figure ES-5a. Ag-NP before sonication (bimodal distribution @ ~33 and ~40 nm)

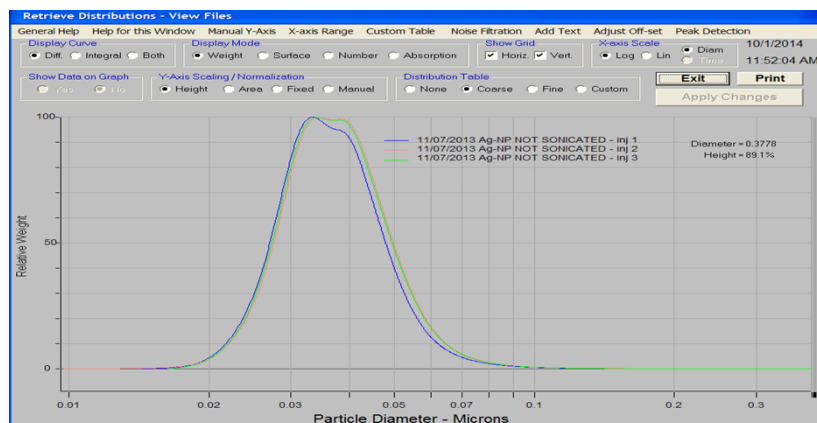


Figure ES-5b. Ag-NP after sonication (highly monodisperse @ ~33 nm)

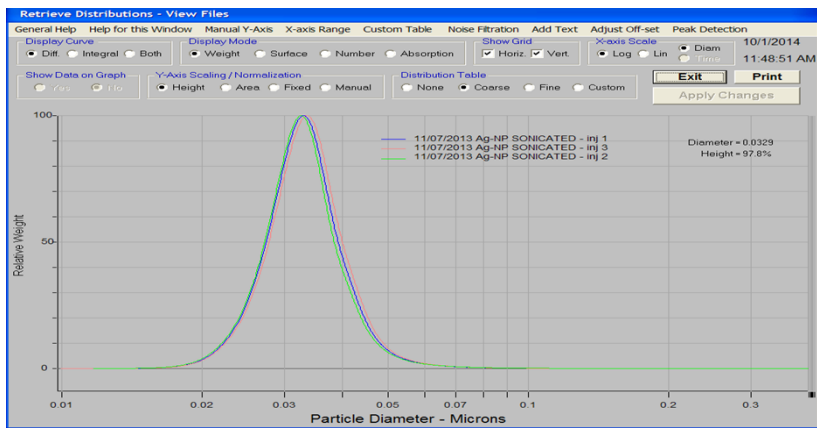
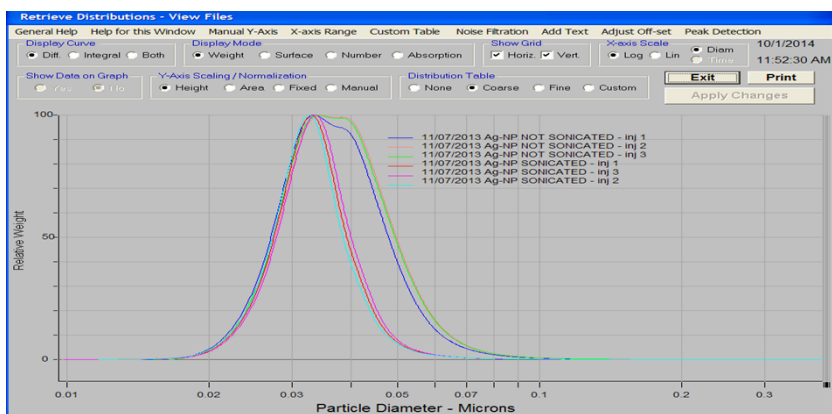


Figure ES-5c. Overlay of plots



ES-4 Construction of a size-based calibration curve, using HDC-ICP-MS data

The theory of HDC allows the size of the eluting particle to be extrapolated from a retention time calibration curve, produced using appropriate sizing standards (5 to 150 nm hydrodynamic diameter). The calibration curve produced in this study, comprised of HDC-ICP-MS data from five gold nanoparticle standards, is presented in Figure ES-6, and was used to calculate that the hydrodynamic radius of the Ag-NP used in the fate/behaviour study. This was confirmed by triplicated analysis of the particles using disc centrifugation analysis.

Figure ES-6 Size (hydrodynamic diameter) calibration curve constructed using HDC-ICP-MS data from five gold nanoparticle standards (citrate-stabilised), analysed in triplicate

